European Journal of Radiology Open 13 (2024) 100578

Contents lists available at ScienceDirect

European Journal of Radiology Open

journal homepage: www.elsevier.com/locate/ejro

Short communication

Reduced dose helical CT scout imaging on next generation wide volume CT system decreases scan length and overall radiation exposure

Alexa E. Golbus [a], John L. Schuzer [b], Chloe Steveson [c], Shirley F. Rollison [d], James Matthews [e], Joseph Henry-Ellis [e], Marco Razeto [e], Marcus Y. Chen [a,*]

[a] Cardiovascular Branch, National Heart, Lung, and Blood Institute, National Institutes of Health, Bethesda, MD, USA
[b] Canon Medical Research USA, Vernon Hills, IL, USA
[c] Canon Medical Systems, Otawara, Tochigi, Japan
[d] Radiology and Imaging Sciences, Clinical Center, National Institutes of Health, Bethesda, MD, USA
[e] Canon Medical Research Europe, Edinburgh, Scotland, UK

ARTICLE INFO

Keywords:
Artificial intelligence
Anatomic landmarks
Radiation dosage
Tomography, spiral computed
Tomography, x-ray computed

ABSTRACT

Purpose: Traditional CT acquisition planning is based on scout projection images from planar anterior-posterior and lateral projections where the radiographer estimates organ locations. Alternatively, a new scout method utilizing ultra-low dose helical CT (3D Landmark Scan) offers cross-sectional imaging to identify anatomic structures in conjunction with artificial intelligence based Anatomic Landmark Detection (ALD) for automatic CT acquisition planning. The purpose of this study is to quantify changes in scan length and radiation dose of CT examinations planned using 3D Landmark Scan and ALD and performed on next generation wide volume CT versus examinations planned using traditional scout methods. We additionally aim to quantify changes in radiation dose reduction of scans planned with 3D Landmark Scan and performed on next generation wide volume CT.

Methods: Single-center retrospective analysis of consecutive patients with prior CT scan of the same organ who underwent clinical CT using 3D Landmark Scan and automatic scan planning. Acquisition length and dose-length-product (DLP) were collected. Data was analyzed by paired t-tests.

Results: 104 total CT examinations (48.1 % chest, 15.4 % abdomen, 36.5 % chest/abdomen/pelvis) on 61 individual consecutive patients at a single center were retrospectively analyzed. 79.8 % of scans using 3D Landmark Scan had reduction in acquisition length compared to the respective prior acquisition. Median acquisition length using 3D Landmark Scan was 26.7 mm shorter than that using traditional scout methods ($p < 0.001$) with a 23.3 % median total radiation dose reduction (245.6 (IQR 150.0–400.8) mGy cm vs 320.3 (IQR 184.1–547.9) mGy cm). CT dose index similarly was overall decreased for scans planned with 3D Landmark and ALD and performed on next generation CT versus traditional methods (4.85 (IQR 3.8–7) mGy vs. 6.70 (IQR 4.43–9.18) mGy, respectively, $p < 0.001$).

Conclusion: Scout imaging using reduced dose 3D Landmark Scan images and Anatomic Landmark Detection reduces acquisition range in chest, abdomen, and chest/abdomen/pelvis CT scans. This technology, in combination with next generation wide volume CT reduces total radiation dose.

1. Introduction

Over 300 million CT examinations are performed worldwide each year, with CT examinations accounting for the primary source of medical radiation exposure [1,2]. Ionizing radiation from CT examinations is a concern due to malignancy risk [3,4]. CT acquisition range parameters are set by radiographers, based on landmarks from anterior-posterior and lateral scout images. Prior studies [5–7] have demonstrated scanning beyond the pre-defined anatomic boundaries of the area of interest in 80–98 % of CT examinations, with most of these extra images

* Correspondence to: Advanced Cardiovascular Imaging Laboratory, Cardiovascular Branch, National Heart, Lung and Blood Institute, National Institutes of Health, 10 Center Drive, Building 10, Room B1D47, Bethesda, MD 20892-1046, USA.
E-mail address: marcus.chen@nih.gov (M.Y. Chen).

https://doi.org/10.1016/j.ejro.2024.100578
Received 27 March 2024; Received in revised form 24 May 2024; Accepted 2 June 2024
2352-0477/© 2024 Published by Elsevier Ltd. This is an open access article under the CC BY-NC-ND license (http://creativecommons.org/licenses/by-nc-nd/4.0/).

providing no additional information [8]. While there have been recent advances in optimization of radiation dose including improved detector capability, automatic exposure control, tube current modulation, iterative reconstruction, and filtration, overscanning remains an issue [2, 9–11]. Overscanning exposes patients to unnecessary excess radiation, with a prior study [7] showing an associated extra dose of 0.6 millisieverts (mSv) for chest CT, 0.5 mSv for abdominal CT, and 1 mSv for chest/abdomen/pelvis CT.

A new scout method utilizing reduced dose helical CT (3D Landark Scan) offers cross-sectional imaging to identify anatomic structures in conjunction with artificial intelligence (AI) assisted automated scan planning using Anatomic Landmark Detection (ALD).

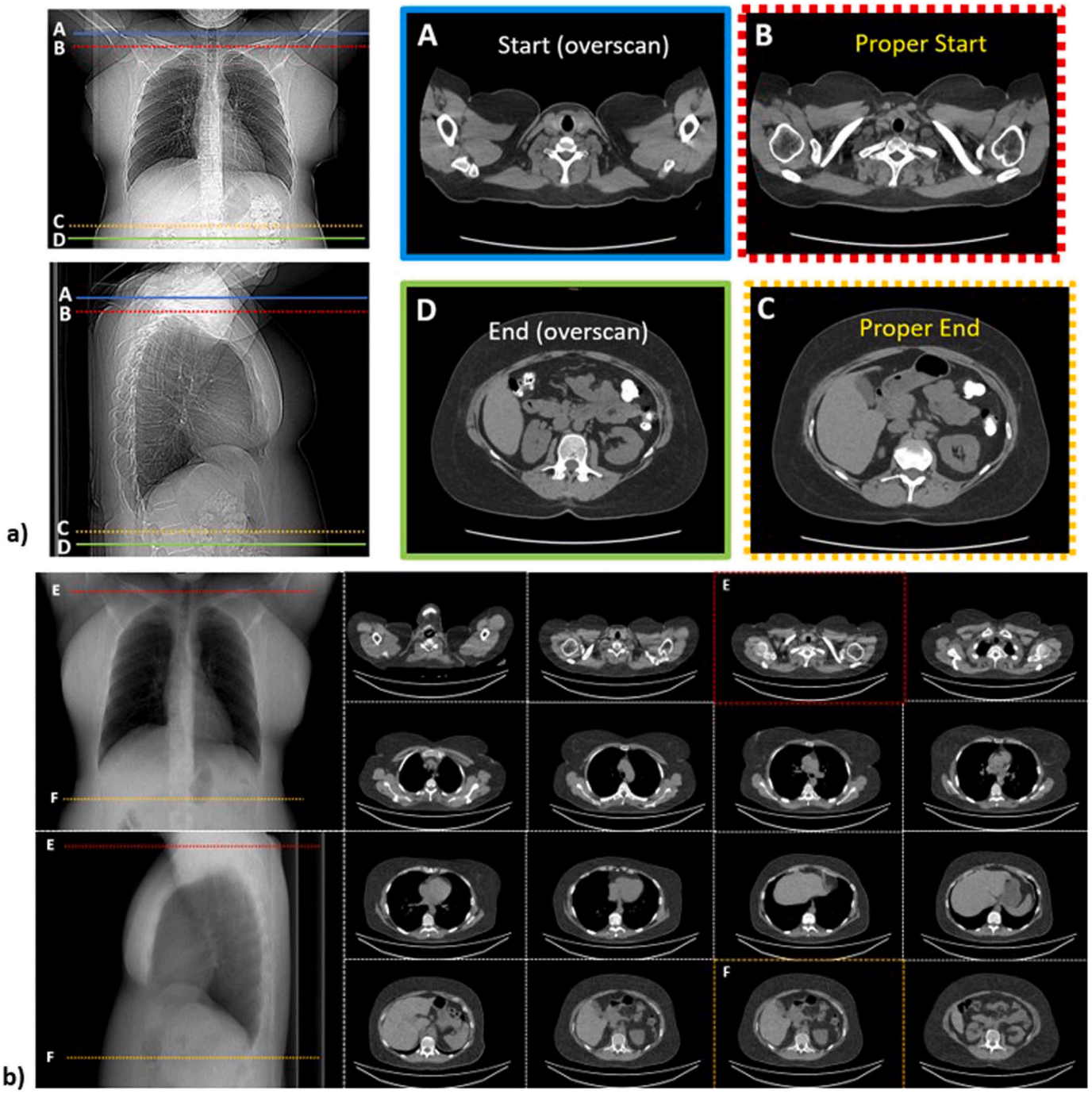

Fig. 1. Traditional and 3D Landmark scout images and scan start/end positions for a chest CT of a 54-year old female. (a) Traditional AP and lateral scout images and start and end scan positions. Lines A and D, and corresponding axial images represent the actual start and end positions of the CT scan planned using traditional scout images where the radiographer estimates the organ locations. Lines B and C and corresponding axial images represent the proper start and end positions for the chest CT to start above the lung apex and go through both adrenal glands. (b) Axial ultra-low dose CT images generated by 3D Landmark scouting and corresponding coronal and lateral projections from the same patient. E and F represent the appropriate start and end positions of the CT planned using the axial 3D Landmark images resulting in a decreased scan length of 34 mm compared to prior imaging (panel a) planned using traditional scout imaging (325 vs 291 mm, respectively). Correspondingly, the radiation dose of the chest CT scan planned by 3D landmark was reduced by 12 % compared to her prior scan planned with traditional scout imaging (249.8 mGy·cm vs 283.7 mGy·cm), representing a 0.47 mSv effective dose savings. Scout image radiation dose itself was reduced by 48 % utilizing 3D Landmark (16.67 vs. 8.67 mGy·cm).

Improved detector capability reduces noise in CT imaging and allows for reductions in radiation dose while preserving image quality [10]. Next generation wide volume CT utilizes a detector that reduces electronic noise, thereby providing the ability to reduce radiation, in addition to the new reduced dose helical CT scout method with ALD.

The purpose of this study is to quantify changes in acquisition length and radiation dose of CT examinations planned automatically using 3D Landmark Scan and ALD and performed on next generation wide volume CT, compared to prior CT exams planned manually using traditional planar anterior-posterior and lateral view scout images.

2. Materials and methods

This retrospective study was considered exempt by the institutional review board, however informed consent to conduct research was priorly obtained for all subjects for use in future studies. 61 consecutive patients with prior CT examination of the same body region that underwent clinical CT planned using 3D Landmark Scan and ALD (Canon Medical Aquilion ONE Insight Edition; Otawara, Tochigi, Japan) at a single center over a 3-month period from 7/17/23–10/16/23 were included in this study. The prior CT examinations were performed on Canon Medical Aquilion ONE Prism Edition, Siemens Somatom Force, Siemens Definition 64, Siemens Somatom Definition Flash, GE Lightspeed VCT, and Philips Brilliance 64.

The 3D Landmark Scan is a reduced dose helical CT (120 kV, 50 mA, pitch 1.5) with SilverBeam Filter. These images are immediately displayed as coronal and sagittal views mimicking traditional scout images and axial 1 mm slice thickness with 1 mm increment reconstructions are displayed (Fig. 1). Anatomic Landmark Detection uses AI to identify landmarks within the images and set the acquisition range and field of view (FOV) based on parameters set in the exam protocol. The radiographer can then manually adjust the acquisition length and FOV if needed. ALD uses AI developed according to the classification forest method detailed in Dabbah et al. [12], which was trained according to a database of landmark ground truth in whole body CT datasets, in order to define 127 anatomical landmarks throughout the body. These anatomical landmarks are used by ALD to automatically set CT examination start/end points [12,13].

Acquisition length, dose-length-product (DLP), and CT dose index (CTDI) were collected from start/end positions and radiation dose summary page. Similarly, DLP was collected for the scout acquisition from the CT scanner produced dose summary page utilizing standard methods [14]. Total radiation dose was calculated as the sum of the radiation dose of the acquisition and radiation dose of the scout image. The effective radiation dose in millisieverts (mSv) was calculated by multiplying dose-length-product by a conversion coefficient (mSv mGy^{-1} cm^{-1}) of 0.014 for chest, 0.015 for abdomen, and 0.0145 for chest/abdomen/pelvis [15]. Paired t-tests were used to determine significant reductions in acquisition length and radiation doses, between the exams planned using 3D Landmark and ALD and performed on next generation wide volume CT and those planned using traditional planar scout images with the radiographers manually selecting the start/end positions of the helical acquisition. Data was further analyzed by subgrouping examinations by body region (chest, abdomen, or chest/abdomen/pelvis). Radiation dose for subgroups was recorded as DLP and CTDI of the diagnostic acquisitions. Data was analyzed by paired t-tests. A p-value less than 0.05 was considered statistically significant.

CT examinations were evaluated for completeness with the definitions of start and end points as follows:

Chest CT begins above the apices of the lungs and scans through the adrenal glands. Abdomen CT begins above the diaphragm and scans through the liver. Chest/abdomen/pelvis CT begins above the apices of the lungs and scans through the symphysis pubis.

Patients with prior scans with no dose page, and therefore no radiation dose data available, were excluded from the radiation analysis. All patients were included in the analysis of acquisition length.

3. Results

3.1. Overall

104 total examinations (48.1 % chest, 15.4 % abdomen, 36.5 % chest/abdomen/pelvis) on 61 individual patients were analyzed with a median time between exams of 461 (IQR 366–1306) days. 83.6 % of patients were female, with mean age 52.0 ± 13.9 years. Patients' mean BMI at the time of the prior scan was 26.3 ± 6.2 kg/m^2, and mean BMI at the time of the recent scan was 26.8 ± 7.3 kg/m^2, with no significant change between the two time points. Exam indication included pulmonary abnormality, malignancy, autoimmune process, immunodeficiency, and infectious process (Table 1). 4 patients only had start/end acquisition positions recorded without a radiation dose page for prior exams; therefore, while 104 exams were included in the analysis of acquisition length, only 100 exams were included in the radiation dose analysis. 74 prior exams were performed on Canon Medical Aquilion ONE Prism Edition, 25 on Siemens Somatom Force, 1 on Siemens Somatom Definition Flash, 1 on Siemens Definition 64, 1 on GE Lightspeed VCT, and 2 on Philips Brilliance 64.

79.8 % of exams planned using 3D Landmark Scan and automatic scan planning with ALD had a reduction in acquisition length compared to the respective prior exam. Median acquisition length using 3D Landmark Scan was 26.7 mm shorter than that planned using traditional scout methods (333.3 (IQR 296.6–625.3) mm vs. 360 (IQR 321.8–645.8) mm, respectively ($p < 0.001$, $n = 104$) (Table 2).

Total dose-length product (scout plus acquisition) for the CT examinations was decreased by 23.3 % for exams using 3D Landmark and ALD compared to traditional scout methods (245.6 (IQR 150.0–400.8) mGy·cm vs. 320.3 (IQR 184.1–547.9) mGy·cm, $p < 0.001$). This corresponded to a total effective dose reduction of 1.2 mSv (Table 2).

DLP for 3D Landmark Scan scout images was lower than DLP for traditional scout images (14.2 (IQR 9.3–16.2) mGy·cm vs. 17.2 (IQR 11.0–28.8) mGy·cm respectively, $p < 0.001$) (Table 2, Fig. 3a).

3.2. Subgroup analysis of scan length according to body region

Median acquisition length for chest CT was 317.3 (IQR 302.3–338) mm for exams planned automatically using 3D Landmark Scan and ALD compared to 330 (IQR 325.8–360)mm for exams planned using traditional scout images ($p < 0.001$, $n = 50$) (Table 2, Fig. 2a). Median acquisition length for abdomen CT was 235.5 (IQR 209.5–246)mm compared to 250 (IQR 240.1–260)mm respectively ($p = 0.003$, $n = 16$) (Table 2, Fig. 2b), and median acquisition length for chest/abdomen/

Table 1
Demographics of 61 patients undergoing a total of 104 CT examinations. Weight and BMI is presented for patients at time of prior CT examination planned with traditional scout imaging ("prior") and at time of recent CT examination planned with 3D Landmark and ALD ("new").

Sample size (n)	61
Gender (%F)	83.6 %
Age (y) (mean ± standard deviation)	52.0 ± 13.9
Height (cm) (mean ± standard deviation)	167.0 ± 8.2
Prior weight (kg) (mean ± standard deviation)	73.4 ± 17.4
Prior BMI (kg/m^2) (mean ± standard deviation)	26.3 ± 6.2
New weight (kg) (mean ± standard deviation)	75.8 ± 22.7
New BMI (kg/m^2) (mean ± standard deviation)	26.8 ± 7.3
Scan Indication	Pulmonary abnormality 49 % (30/61), Malignancy 23 % (14/61), Autoimmune 18 % (11/61), Immunodeficiency 7 % (4/61), Infectious 3 % (2/61)

Table 2
Scan lengths and radiation doses for 104 CT examinations planned using traditional scout imaging ("prior") and planned using 3D Landmark and ALD ("new"). Radiation doses presented as dose length product (DLP), effective dose (in milisieverts), and CT dose index (CTDI). Total DLP and CTDI reflect the sum of the scout imaging dose and acquisition dose. Scan lengths, DLP and corresponding effective doses of diagnostic acquisitions are further broken into subgroup by body region. Effective radiation dose in millisieverts (mSv) was calculated from the DLP using a k factor of 0.014 for chest, 0.015 for abdomen, and 0.0145 for chest/abdomen/pelvis [13]. Data represented as median and interquartile range. n = 50 for chest CT scan length, n = 16 for abdomen scan length, n = 38 for chest/abdomen/pelvis scan length, and n = 104 for scout scan length. n = 49 for chest radiation doses, n = 15 for abdomen radiation doses, n = 36 for chest/abdomen/pelvis radiation doses, and n = 100 for scout radiation doses.

	Scan Length (mm)			DLP (mGy cm)			Effective dose (mSv)			CTDI (mGy)		
	New	Prior	p-value	New	Prior	p-value	New	Prior	p-value	New	Prior	p-value
Total examination (acquisition + scout)	–	–	–	245.6 (IQR 150.0–400.8)	320.3 (IQR 184.1–547.9)	p < 0.001	3.4 (IQR 2.1–5.9)	4.64 (IQR 2.6–7.9)	p < 0.001	–	–	–
Overall diagnostic acquisition	333.3 (IQR 296.6–625.3)	360 (IQR 321.8–645.8)	p < 0.001	232.7 (IQR 140.6–385.5)	310.4 (164.1–535.5)	p < 0.001	3.3 (IQR 2.0–5.6)	4.5 (IQR 2.4–7.5)	p < 0.001	4.85 (IQR 3.8–7.0)	6.7 (IQR 4.4–9.2)	p < 0.001
Chest acquisition	317.3 (IQR 302.3–338.0)	330.0 (IQR 325.8–360)	p < 0.001	160.4 (IQR 133.8–223.6)	182.1(IQR 146–283.7)	p = 0.007	2.3(IQR 1.9–3.1)	2.6 (IQR 2.0–3.9)	p = 0.007	4.4 (IQR 3.6–6.9)	4.6 (IQR 3.7–7.6)	p = 0.12
Abdomen acquisition	235.5 (IQR 209.5–246)	250 (IQR 240.1–260)	p = 0.003	124.9 (IQR 96.8–166.8)	236.8 (IQR 178.1–284.6)	p = 0.004	1.9 (IQR 1.5–2.5)	3.6 (IQR 2.7–4.3)	p = 0.004	4.4 (IQR 4.0–6.3)	7.7 (IQR 6.5–8.8)	p = 0.009
Chest/abdomen/pelvis acquisition	635 (IQR 625–667.3)	660 (IQR 641.3–687.3)	p < 0.001	379.7 (IQR 319.0–531.8)	531.6 (IQR 465.4–689.2)	p = 0.001	5.5 (IQR 4.6–7.7)	7.7 (IQR 6.8–10.0)	p = 0.001	5.6 (IQR 4.6–7.3)	7.5 (IQR 6.4–9.6)	p = 0.002
Scout acquisition	610.0 (IQR 378–699)	627.0 (IQR 387.8–717.0)	p = 0.07	14.2 (IQR 9.3–16.2)	17.2 (IQR 11.0–28.8)	p < 0.001	0.21 (IQR 0.13–0.24)	0.24 (IQR 0.16–0.42)	p < 0.001	–	–	–

pelvis CT was 635 (IQR 625–667.3)mm compared to 660 (IQR 641.3–687.3)mm respectively ($p < 0.001$, $n = 38$) (Table 2, Fig. 2c).

3.3. Subgroup analysis of radiation dose according to body region

DLP, CTDI, and effective doses for chest, abdomen, and chest/abdomen/pelvis CT acquisitions are presented in Table 2 and Fig. 3. DLP for chest CT acquisitions was reduced by 11.9 %, corresponding to a 0.3 mSv reduction in effective dose ($p = 0.007$). DLP for abdomen acquisitions was reduced by 47.3 %, corresponding to a 1.7 mSv reduction in effective dose ($p = 0.004$). DLP for chest/abdomen/pelvis acquisitions was reduced by 28.6 %, corresponding to a 2.2 mSv reduction in effective dose ($p = 0.001$).

4. Discussion

In our study, we evaluated the reduction in acquisition length and radiation dose for CT examinations planned automatically using 3D Landmark Scan and ALD and performed on next generation wide volume CT, compared to exams planned manually using traditional scout images. No prior study has evaluated the ability to reduce CT acquisition length by optimizing acquisition planning using low-dose helical scout imaging in combination with artificial intelligence assisted automatic scan planning. Acquisition length was reduced overall by 26.7 mm and total radiation dose of the examination was reduced by 23.3 %. All subgroups, classified by body region of CT exam (chest, abdomen, or chest/abdomen/pelvis) had a significant reduction in acquisition length and a reduction in radiation dose of the diagnostic acquisition, ranging from 0.3 to 2.2 mSv.

The results demonstrate that acquisition planning using reduced dose 3D Landmark Scan and automatic scan planning with ALD for chest, abdominal, and chest/abdomen/pelvis CT exams reduces acquisition range. This reduction in acquisition length in combination with the radiation reduction provided by next generation CT allows for a significant reduction in radiation dose. Further, by using an additional silver filter, the 3D Landmark helical scout imaging exposed patients to a lower radiation dose than that of traditional scout imaging.

Prior studies [5–8] have found that a significant proportion of CT studies scan beyond the anatomical boundaries ("overscan"). Although there are protocols with pre-defined anatomical boundaries that exams are planned off of based on scout images, radiographers may err on the side of overscanning to avoid truncating relevant anatomy and potentially missing a pathologic finding [5]. A prior study by Liao et al. [5] evaluating overscanning found a mean extra acquisition length of 43.2 mm with a corresponding increase in DLP, and suggested that a low dose localizer image would be useful to obtain in cases where anatomic boundaries could not be definitively seen on scout imaging. Our study used low-dose cross sectional imaging in the place of these traditional 2D scout images to set acquisition boundaries. While these prior studies demonstrate that overscanning is prevalent in CT imaging, our study adds to this by providing an analysis of the actual scan length reduction achieved in clinical practice when utilizing helical scout imaging and artificial intelligence assisted automatic scan planning. While we were not analyzing whether traditional scout imaging exceeded the predefined anatomical boundaries, as these prior studies did, we instead compared acquisition lengths of imaging obtained from scout images that utilized cross-sectional imaging in conjunction with artificial intelligence, to that of traditional scout imaging, for each patient. In our study, any difference between the acquisition length obtained from traditional scout images versus 3D Landmark images represented extra unnecessary length, and we similarly found that traditional scout images resulted in additional acquisition length.

Further, manual CT scan planning is subject to interpersonal variation between radiographers, however, automatic scan planning with Anatomic Landmark Detection eliminates such variability.

While the reduction in radiation dose found in our study is due to a

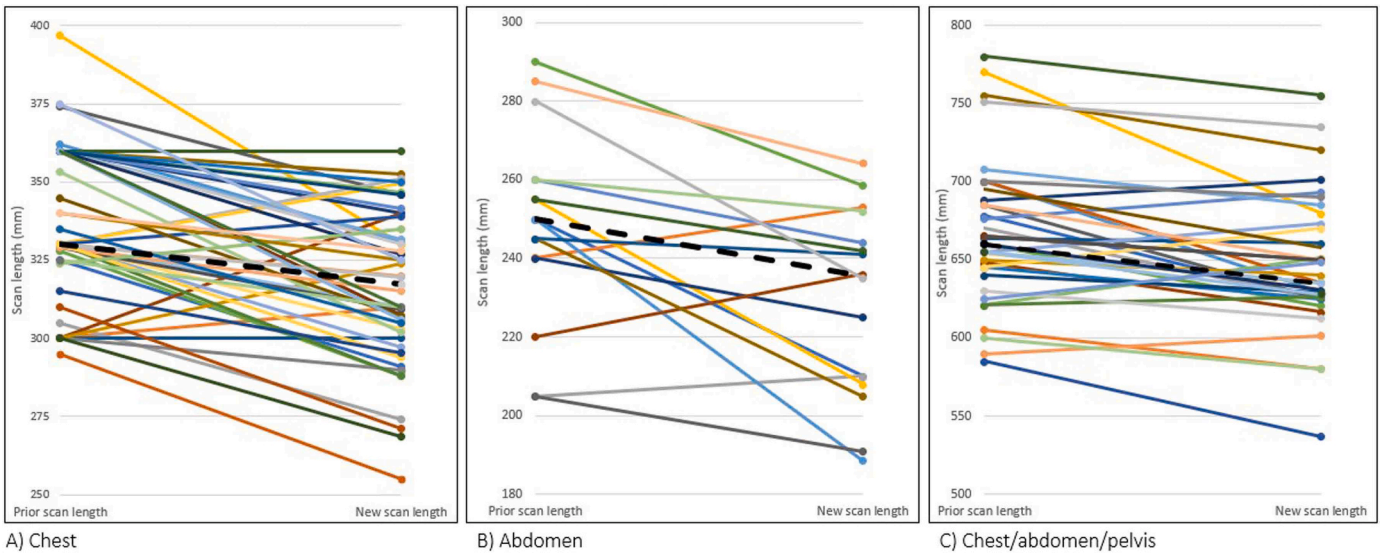

Fig. 2. Scan length (mm) for (a) chest, (b), abdomen, and (c) chest/abdomen/pelvis CT exams planned using 3D Landmark Scan and Anatomic Landmark Detection versus those planned using traditional scout images. (a) Median scan length 317.3 (IQR 302.3–338)mm compared to 330 (IQR 325.8–360)mm, respectively ($p < 0.001$, $n = 50$). Median reduction of 12.7 mm represented by the black dashed line. (b) Median scan length 235.5 (IQR 209.5–246)mm compared to 250 (IQR 240.1–260)mm respectively($p = 0.003$, $n = 16$). Median reduction of 14.5 mm represented by the black line. (c) Median scan length 635 (IQR 625–667.3)mm compared to 660 (IQR 641.3–687.3)mm respectively ($p < 0.001$, $n = 38$). Median reduction of 25.0 mm represented by the black line.

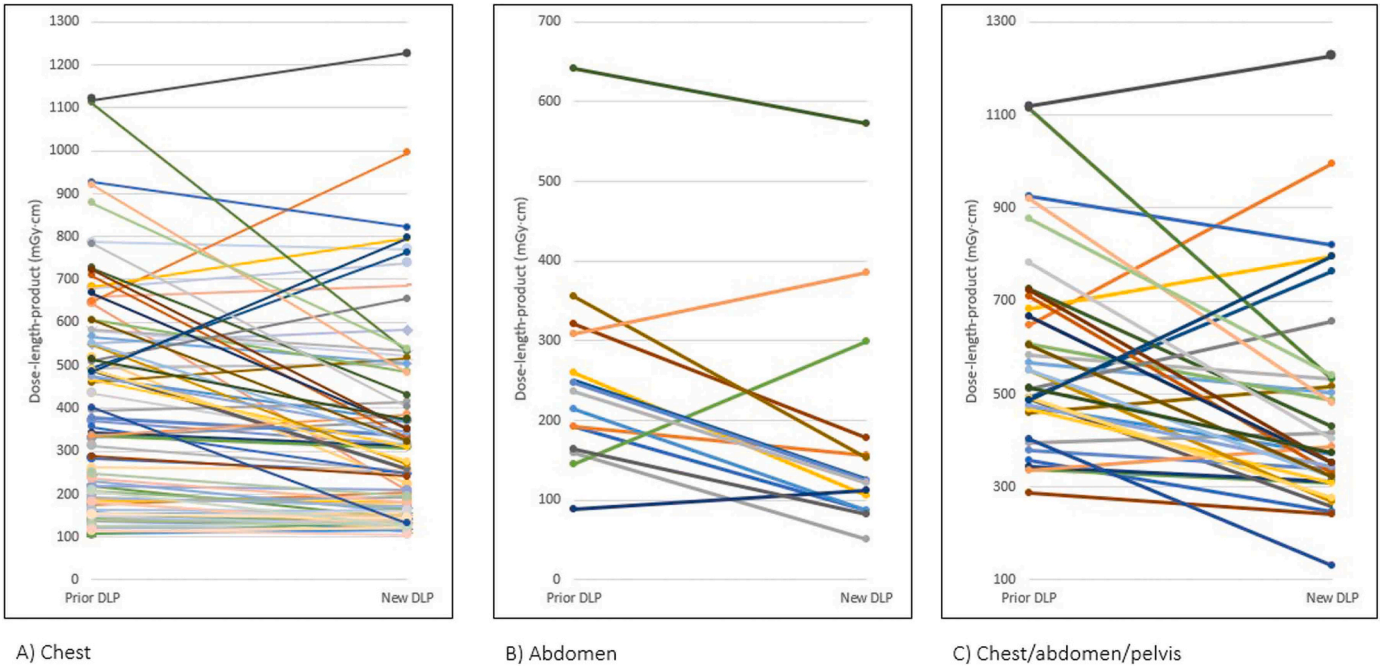

Fig. 3. Dose-length product (DLP) (mGy·cm) for (a) chest, (b) abdomen, and (c) chest/abdomen/pelvis CT exams planned using 3D Landmark Scan and Anatomic Landmark Detection and performed on next generation CT ("new DLP") versus those planned using traditional scout methods ("prior DLP"). (a) Median DLP for chest CT was reduced by 11.9 %, from 182.1 (IQR 146.1–283.7) to 160.4 (IQR 133.8–223.6) mGy·cm, $p = 0.007$, $n = 49$. (b). Median DLP for abdomen CT was reduced by 47.3 % from 236.8 (IQR 178.1–284.60) to 124.9 (96.8–166.8) mGy·cm, $p = 0.004$, $n = 15$. (c) Median DLP for chest/abdomen/pelvis CT was reduced by 28.6 %, from 531.6 (IQR 465.4–689.2) to 379.7 (IQR 319.0–531.8) mGy·cm, respectively, $p = 0.001$, $n = 36$.

combination of both decreased acquisition length and next generation CT technology, we found a reduction in effective radiation dose of the diagnostic acquisition ranging from 0.3 to 2.2 mSv, depending on body region. Prior studies [6–8] have found overscanning exposes patients to similar excess radiation doses, with Zanca et al. reporting an associated 0.5–1 mSv of additional exposure.

No anatomy was missed or underscanned with scans planned using 3D Landmark Scan and ALD. While some scans planned using this technology still scanned beyond the anatomical boundaries, overall, overscanning was significantly improved when using 3D Landmark and ALD. One patient with an increase in acquisition length had a prior CT that prematurely truncated pertinent anatomy.

This was a single center study and only evaluated chest, abdomen, and chest/abdomen/pelvis CT scans. We were unable to isolate the exact dose reduction attributable to decreased scan length versus the reduction afforded by the improved detector capability of the next generation

wide volume CT scanner. This study reflects the early adoption of a new technology and further optimization of scan length with 3D Landmark and ALD is possible.

5. Conclusions

CT examinations performed on next generation wide volume CT and planned with 3D Landmark Scan and ALD reduced CT acquisition length by a median of 26.7 mm and provided an overall 23.3 % reduction in radiation dose.

Ethics Statement

All research was performed in compliance with relevant laws and institutional guidelines.

Ethical approval

This retrospective study was considered exempt by the institutional review board, however informed consent to conduct research was obtained for all subjects.

Funding

This work was supported by the Intramural Research Program, National Institutes of Health (NIH), National Heart, Lung, and Blood Institute (Bethesda, MD). This work was also made possible by the NIH Medical Research Scholars Program, a public-private partnership supported jointly by the NIH and contributions to the Foundation for the NIH from private donors.

CRediT authorship contribution statement

James Matthews: Writing – review & editing, Software. **Marco Razeto:** Writing – review & editing, Software. **Joseph Henry-Ellis:** Writing – review & editing, Software. **Marcus Y. Chen:** Writing – review & editing, Writing – original draft, Supervision, Funding acquisition, Formal analysis, Data curation, Conceptualization. **Shirley F. Rollison:** Writing – review & editing, Investigation. **Chloe Steveson:** Writing – review & editing, Methodology, Conceptualization. **John L. Schuzer:** Writing – review & editing, Methodology, Conceptualization. **Alexa E. Golbus:** Writing – review & editing, Writing – original draft, Visualization, Formal analysis, Data curation, Conceptualization.

Declaration of Competing Interest

The authors declare the following financial interests/personal relationships which may be considered as potential competing interests: John Schuzer and Chloe Steveson are employees of Canon Medical, but did not participate in data collection or analysis. James Matthews, Joseph Henry-Ellis, and Marco Razeto are employees of Canon Medical Research, but did not participate in data collection or analysis. No other authors declare conflicts of interest.

Acknowledgements

This work was supported by the Intramural Research Program, National Institutes of Health (NIH), National Heart, Lung, and Blood Institute (Bethesda, MD) [grant # 1ZIAHL006220]. This work was also made possible by the NIH Medical Research Scholars Program, a public-private partnership supported jointly by the NIH and contributions to the Foundation for the NIH from private donors.

References

[1] L. Schockel, G. Jost, P. Seidensticker, P. Lengsfeld, P. Palkowitsch, H. Pietsch, Developments in X-ray contrast media and the potential impact on computed tomography, Invest Radio. 55 (2020) 592–597.
[2] Y. Salimi, I. Shiri, A. Akhavanallaf, et al., Deep learning-based fully automated Z-axis coverage range definition from scout scans to eliminate overscanning in chest CT imaging, Insights Imaging 12 (2021) 162.
[3] N.D. Farrell, J.H. Dooley, B.W. Sheffer, J.R. Sawyer, D.M. Kelly, Radiation exposure in multiple hereditary exostoses: a retrospective review, J. Orthop. 40 (2023) 87–90.
[4] H. Osman, M. Alosaimi, F. Alghamdi, et al., Evaluation of CT dose and establishment of local DRLs for abdomen pelvis examinations in hospitals in Taif City, Saudi Arabia, Rad. Phys. Chem. (2022) 202.
[5] E.A. Liao, L.E. Quint, M.M. Goodsitt, I.R. Francis, S. Khalatbari, J.D. Myles, Extra Z-axis coverage at CT imaging resulting in excess radiation dose: frequency, degree, and contributory factors, J. Comput. Assist Tomogr. 35 (2011) 50–56.
[6] J. Campbell, M.K. Kalra, S. Rizzo, M.M. Maher, J.A. Shepard, Scanning beyond anatomic limits of the thorax in chest CT: findings, radiation dose, and automatic tube current modulation, AJR Am. J. Roentgenol. 185 (2005) 1525–1530.
[7] F. Zanca, M. Demeter, R. Oyen, H. Bosmans, Excess radiation and organ dose in chest and abdominal CT due to CT acquisition beyond expected anatomical boundaries, Eur. Radiol. 22 (2012) 779–788.
[8] M.K. Kalra, M.M. Maher, T.L. Toth, R.S. Kamath, E.F. Halpern, S. Saini, Radiation from "extra" images acquired with abdominal and/or pelvic CT: effect of automatic tube current modulation, Radiology 232 (2004) 409–414.
[9] M.M. Rehani, Radiological protection in computed tomography and cone beam computed tomography, Ann. ICRP 44 (sup_1) (2015) 229–235.
[10] M. May, R. Heiss, J. Koehnen, et al., Personalized chest computed tomography: minimum diagnostic radiation dose levels for the detection of fibrosis, nodules, and pneumonia, Invest Radio. 57 (2022) 148–156.
[11] L. Yu, X. Liu, S. Leng, J.M. Kofler, J.C. Ramirez, M. Qu, J. Christner, J.G. Fletcher, C.H. McCollough, Radiation dose reduction in computed tomography: techniques and future perspective, Imaging Med 1 (1) (2009) 65–84.
[12] M.A. Dabbah, S. Murphy, H. Pello, R. Courbon, E. Beveridge, S. Wiseman, D. Wyeth, I. Poole, Detection and location of 127 anatomical landmarks in diverse datasets, Med. Imaging (2014).
[13] A. O'Neil, S. Murphy, I. Poole, Anatomical Landmark Detection in CT Learned Atlas Location Autocontext, MIUA (2015) 189–194.
[14] International Electrotechnical Commission. (2016). *Medical electrical equipment-Part 2-44: Particular requirements for the basic safety and essential performance of x-ray equipment for computed tomography* (IEC Standard 60601-2-44).
[15] American Association of Physicists in Medicine Task Group 23: CT Dosimetry. (2008). The measurement, reporting, and management of radiation dose in CT. College Park (MD): American Association of Physicists in Medicine.